Supporting Information

A New Strategy for Specific Eradication of Implant-Related Infections Based on Special and Selective Degradability of Rhenium Trioxide Nanocubes

Wenlong Zhang,[†,#] Chuang Yang,[§,#] Ziyu Lei,[†] Guoqiang Guan,[†] Shu-ang He,[†] Zhenbo Zhang,[ǀ] Rujia Zou,[‡,*] Hao Shen,[§,*] and Junqing Hu[†,*]

[†]State Key Laboratory for Modification of Chemical Fibers and Polymer Materials, International Joint Laboratory for Advanced Fiber and Low-dimension Materials, College of Materials Science and Engineering, Donghua University, Shanghai, 201620, China

[‡]College of Health Science and Environmental Engineering, Shenzhen Technology University, Shenzhen, 518118, China

[§]Department of Orthopaedics, Shanghai Jiao Tong University Affiliated Sixth People's Hospital, Shanghai Jiao Tong University, Shanghai 200233, China

[ǀ]Reproductive Medicine Center, Department of Obstetrics and Gynecology, Shanghai General Hospital, Shanghai Jiaotong University, Shanghai, 200080, China

*E-mail: rjzou@dhu.edu.cn; shenhao7212@sina.com; hu.junqing@dhu.edu.cn

[#]These authors contributed equally to this work.

Details for MATERIALS AND METHODS:

1. Fabrication and Characterization of rhenium trioxide (ReO_3) nanocubes (NCs). The fabrication and characterization of ReO_3 NCs were according to our previous report.[1] Rhenium (VII) oxide (Re_2O_7, 99.99%) was obtained from Aladdin Reagent Co. Ltd. (Shanghai, China). Methanol (≥ 99.5%) was purchased from Sinopharm Chemical Reagent Co., Ltd. (Shanghai, China). All chemicals were used as received.

ReO_3 NCs were fabricated through a simple space-confined on-substrate reaction approach according to our previous report.[1] Briefly, 300 μL of 0.1 M freshly prepared Re_2O_7 methanolic solution was uniformly sandwiched between two halves of silicon wafer as substrates cut from a complete 4-inch (100) monocrystalline silicon wafer. Then, this Re_2O_7 methanolic solution between substrates was treated at 250 ^oC for 5 min and changed into a red thin film with metallic luster, indicating the formation of the ReO_3 NCs on the silicon wafer substrates. Subsequently, the substrates loading ReO_3 NCs were placed in 20 mL of methanol and sonicated for 15 min, so that the ReO_3 NCs were separated from substrates. The resulting bluish green methanol suspension was centrifugated at 1000 rpm for 5 min to get rid of bigger and aggregated nanoparticles and the supernatant was carefully collected. After that, the collected supernatant was centrifuged at 13000 rpm for 10 min and washed several times with methanol using the same method. The obtained bluish green precipitate was dried in vacuum at 70 ^oC for 24 h to form the final product of red ReO_3 NCs (Figure S1).

SEM images were acquired on a scanning electron microscope (S-4800), and TEM images were taken on a transmission electron microscope (JEM-2100F). XRD measurement was conducted with a D/max-2550 PC X-ray diffractometer (Rigaku). UV-Vis-(near infrared) NIR absorption spectra were obtained by UV-Vis 1901 spectrophotometer (Phoenix). Concentrations

of Re ions were determined *via* a Leeman Laboratories Prodigy high dispersion inductively coupled plasma atomic emission spectroscopy (ICP-AES).

2. Photothermal Performance of ReO_3 NC Aqueous Dispersions. The assessment of photothermal performance for the aqueous dispersions of ReO_3 NCs was performed according to our previous report.[1] To measure the photothermal effect, the ReO_3 NC aqueous dispersions (100 μL) with various Re ion concentrations (*i.e.*, 0, 12.5, 25, 50, 100 and 200 ppm) were irradiated by the 808 nm NIR laser (Shanghai Xilong Optoelectronic Technology Co., Ltd., China) at a power density of 0.7 W/cm^2 with a working distance of 20 cm and a spot area of ~0.38 cm^2 for 3 min. The temperature was monitored and imaged meanwhile by a thermal imaging camera (FLIR A300, USA).

3. *In Vitro* Cytotoxicity Evaluation. The evaluation for *in vitro* cytotoxicity of the ReO_3 NCs was conducted according to our previous report.[1,2] Rat bone marrow mesenchymal stem cells (rBMSCs) obtained from Stem Cell Bank of Chinese Academy of Sciences (Shanghai, China) were cultured in Dulbecco's modified Eagle's medium (DMEM) (GIBCO, Grand Island, NY, USA), supplemented with 10% fetal bovine serum (FBS, GIBCO) and 1% penicillin/streptomycin in T175 (Corning, NY, USA) at a concentration of 2×10^5 cells per mL. The cells were incubated in a humidified atmosphere of 5% CO_2 at 37 ^{o}C to cultivate cells *in vitro*. For *in vitro* cytotoxicity test, rBMSCs were seeded into 96-well cell culture plates (5×10^3 cells per well). After 24 h, the top layer of the medium was exchanged with medium containing the ReO_3 NCs' solution with different Re ion concentrations (*i.e.*, 0, 25, 50, 100, 200 and 400 ppm) before and after degradation dispersed by ultrasound in DMEM. After another 24 h, 10% CCK8 (Dojindo Laboratories, Kumamoto, Japan) solution was added to each well, according to the manufacturer's instructions. Data were collected from three separated experiments with four

replications each. Before comparison, the absorbance was normalized to that of a control group without the ReO_3 NCs.

4. Hemolysis Assay. The hemolysis assay for the ReO_3 NCs was performed according to our previous report.[1] Red blood cells were obtained from ethylene diamine tetraacetic acid (EDTA)-stabilized blood from health mice and then washed several times with phosphate buffered saline (PBS, pH 7.4). The diluted cell suspension (20% in PBS) was mixed with ReO_3 NCs' solution at different Re ion concentrations (*i.e.*, 62.5, 125, 250, 500 and 1000 ppm). The deionized water and PBS were used as positive and negative controls. All the samples were maintained at room temperature for 4 h. Then, the mixtures were centrifuged and the supernatants were collected for microplate reader measurement at 570 nm.

5. *In Vitro* Photothermal Anti-Biofilm. For real-time polymerase chain reaction (RT-PCR) analysis of related gene transcription for *S. aureus* biofilms, the genes involving forming *S. aureus* biofilms were quantitatively tested *via* RT-PCR according to our previous report.[3] The adhering bacteria were collected and pelleted by centrifugation at 10000 rpm for 5 min and then resuspended in 1 mL of PBS with 10^5 ppm lysostaphin (Sigma) and incubated for 10 min at 37 ^{o}C. Total RNA extraction was conducted through the RNeasy Mini Kit (Qiagen, Germany). Afterwards, 1 μg of the total RNA was reverse transcribed to its complementary DNA (cDNA) *via* the PrimeScript RT reagent kit (Takara), and RT-PCR analysis was performed on a Bio-Rad C1000 system using SYBR Premix Ex Taq II (Takara). Commercially fabricated primers related to the target genes were used, as presented in Table S1. The expression levels of icaA, fnbA, atlE and sarA were appraised and normalized with respect to that of the internal standard gene 16S rRNA. The quantification of the expression of the target genes was grounded on a cycle threshold value for each sample that was computed by averaging three replicate measurements.

6. *In Vivo* Toxicity, Biodistribution and Metabolism. *In Vivo* toxicity, biodistribution and metabolism were carried out according to our previous report.[1] Healthy BALB/c mice were i.v. injected with the ReO_3 NCs (20 mg/kg, 200 μL) and euthanized at the 1st, 3rd, 7th, 15th and 30th day (five mice per time point) post injection. Another five healthy BALB/c mice were used as the control. Before the mice were euthanatized, blood samples (~1 mL) were collected for blood biochemistry and complete blood panel analyses. Major organs of those mice were dissected and divided into two halves for histological examination and biodistribution measurement, respectively. For histological examination, the major organs including heart, liver, spleen, lung and kidney were dissected from each mouse, to make paraffin sections for further H&E staining, and then examined by a Leica DMi8 fluorescence microscope. For biodistribution measurement, major organs including heart, liver, spleen, lung, kidney, stomach, intestine, skin, muscle and bone from the mice were solubilized by aqua regia for ICP-AES measurement to determine the Re content in these different organs. Additionally, another five healthy BALB/c mice i.v. injected with the ReO_3 NCs (20 mg/kg, 200 μL) were raised in the metabolism cages. Urine and feces of each mouse were collected at different time points, and then solubilized by aqua regia for ICP-AES measurement to determine the Re content in each sample.

Table S1. Primers used in the present study for real-time polymerase chain reaction.

Target gene	Direction	Primer sequence (5'→3')
icaA	F	TGCTGGCGCAGTCAATACTA
icaA	R	CATGGCAAGCGGTTCATACT
fnbA	F	GTCAAGTTATGGCGACAGGA
fnbA	R	GCGTCACTGTTGTAGGATCA
sarA	F	GCAATTACAAAAATCAATGATTGC
sarA	R	AGTTCAATTTCGTTGTTTGCTTCA
atlE	F	TATCGGTTTGCTTTTGTTGG
atlE	R	AGGATGGATTGCTGCTAAGG
16S rRNA	F	TCGTGTCGTGAGATGTTGGGTTA
16S rRNA	R	GGTTTCGCTGCCCTTTGTATTGT

Table S2. Summary of degradability for current degradable inorganic photothermal nanoagents.

Degradable inorganic photothermal nanoagents	A/A_0 or C/C_0 (%)	Time	Condition	Ref.
ReO_3 nanocubes	0.7	3 h	λ_{max}, PBS, pH 7.4	1
Bare black phosphorus quantum dots	~15	24 h	λ_{max}, PBS, pH 7.4	4
Bare ultrasmall black phosphorus nanosheets	45	72 h	450 nm, aqueous solution	5
Black phosphorus@hydrogel	~27	1 h	λ_{max}, aqueous solution, NIR light irradiation	6
MoO_x nanosheets	~8	4 h	λ_{max}, PBS, pH 7.4	7
$MoTe_2$ nanosheets	~35	30 min	λ_{max}, aqueous solution, NIR light irradiation	8
Co_3O_4 nanoprisms	~100	30 days	λ, PBS, pH 7.4, without H_2O_2	9
Co_3O_4 nanoparticles	~100	10 min	λ, aqueous solution, pH 7.5, without ascorbic acid	10
VS_2 nanodots	~57	30 days	λ_{max}, aqueous solution	11
Cu@Cu_2O@polymer nanoparticles	~100	7 days	λ_{max}, aqueous solution, without H_2O_2	12
MoS_2 nanoflakes	21	1 day	808 nm, PBS, pH 7.4	13
Fe_3S_4 tetragonal nanosheets	-	-	-	14
ReO_3 nanocubes	5.2	3 h	λ_{max}, PBS, pH 7.4	This work

Figure S1. A photo of solid ReO_3 NC thin film on glass substrate.

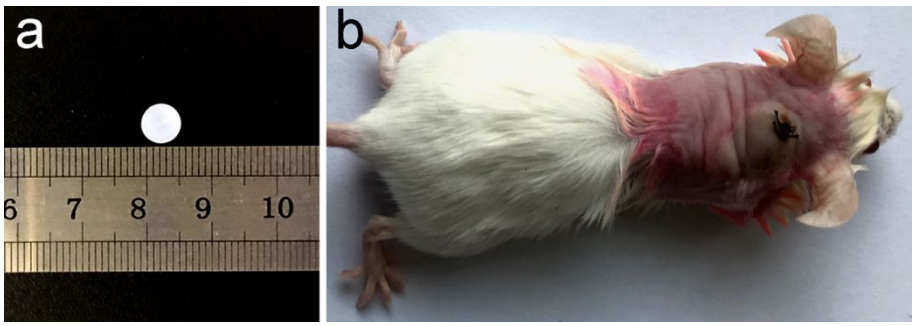

Figure S2. Photos of (a) polyethylene washer and (b) mouse implant-related soft tissue infection model.

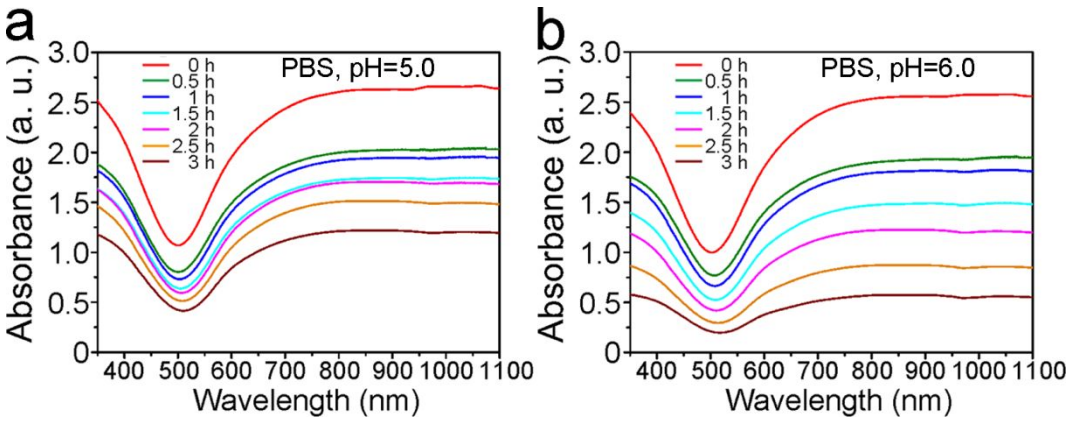

Figure S3. UV-Vis-NIR absorption spectra of ReO_3 NCs over time in PBS (166 ppm) with (a) pH 5.0 and (b) pH 6.0.

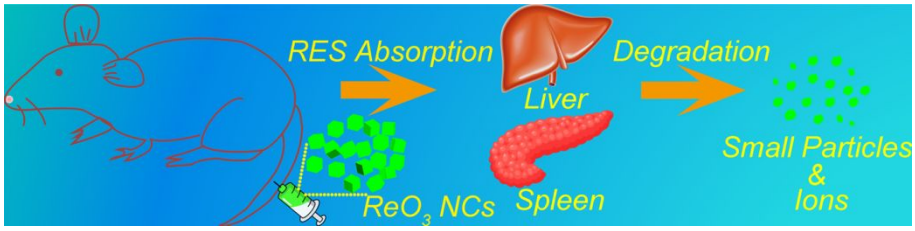

Figure S4. Illustration to describe the *in vivo* degradation and clearance process of the ReO_3 NCs.

As suggested, the nanomaterials could be quickly cleared *via* the kidney when they are small enough in their size,[15,16] while larger-sized ones may go through a slower excretion from the RES. From this result in our work, it is deduced that the ReO_3 NCs after being phagocytosed by the Kupffer cells and spleen macrophages, might be gradually oxidized and degraded into small nanoparticles or $[ReO_4]^-$ ions to facilitate such effective clearance from the RES (Figure S4).[1,7,11,17]

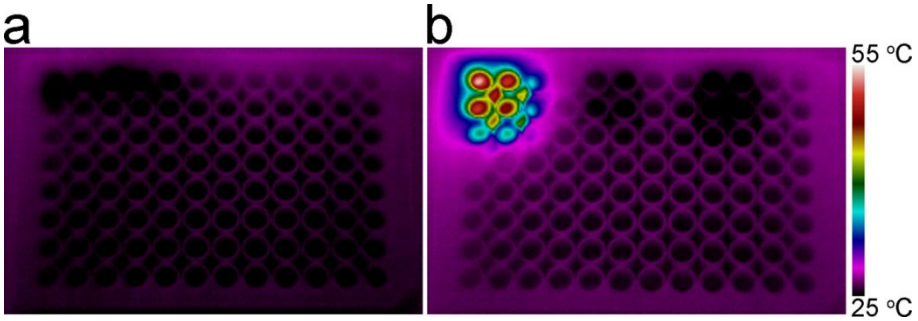

Figure S5. IR thermal images of 96-well plates when the wells are incubated with ReO_3 NCs and planktonic bacteria (a) before and (b) after exposure to an 808 nm laser.

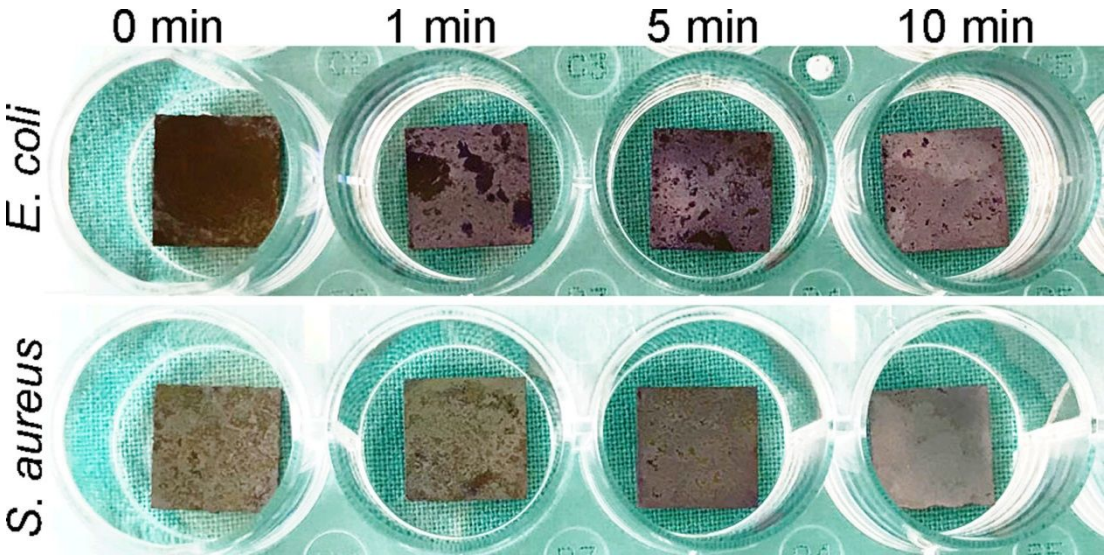

Figure S6. Photos for crystal violet staining of *E. coli* and *S. aureus* biofilms on the titanium metal plate surfaces treated with the ReO_3 NCs after exposure to 808 nm laser irradiation (0.7 W/cm^2) for different times.

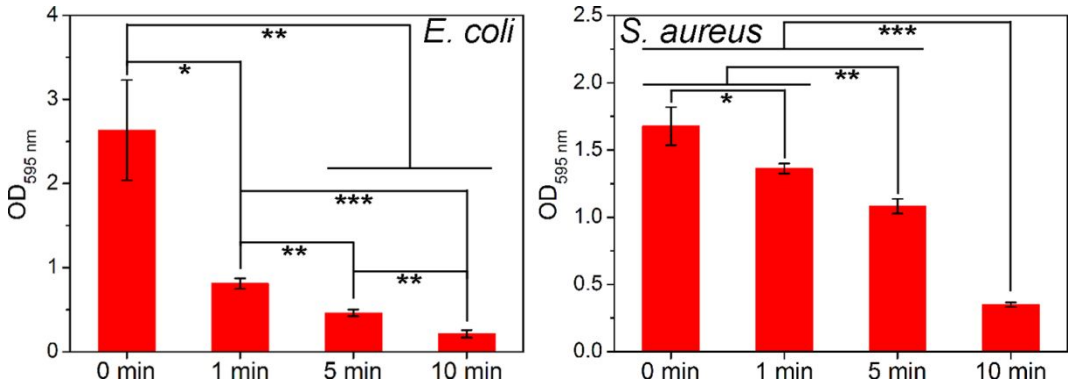

Figure S7. OD at 595 nm for *E. coli* and *S. aureus* biofilms washed out after crystal violet staining.

References:

(1) Zhang, W. L.; Deng, G. Y.; Li, B.; Zhao, X. X.; Ji, T.; Song, G. S.; Xiao, Z. Y.; Cao, Q.; Xiao, J. B.; Huang, X. J.; Guan, G. Q.; Zou, R. J.; Lu, X. W.; Hu, J. Q. Degradable Rhenium Trioxide Nanocubes with High Localized Surface Plasmon Resonance Absorbance like Gold for Photothermal Theranostics. *Biomaterials* **2018**, *159*, 68-81.

(2) Zhang, W. L.; Xiao, J. B.; Cao, Q.; Wang, W. H.; Peng, X.; Guan, G. Q.; Cui, Z.; Zhang, Y. F.; Wang, S. G.; Zou, R. J.; Wan, X. J.; Qiu, H. L.; Hu, J. Q. An Easy-To-Fabricate Clearable CuS-Superstructure-Based Multifunctional Theranostic Platform for Efficient Imaging Guided Chemophotothermal Therapy. *Nanoscale* **2018**, *10*, 11430-11440.

(3) Wang, J. X.; Li, J. H.; Guo, G. Y.; Wang, Q. J.; Tang, J.; Zhao, Y. C.; Qin, H.; Wahafu, T.; Shen, H.; Liu, X. Y.; Zhang, X. L. Silver-Nanoparticles-Modified Biomaterial Surface Resistant to Staphylococcus: New Insight into the Antimicrobial Action of Silver. *Sci. Rep.* **2016**, *6*, 32699.

(4) Shao, J. D.; Xie, H. H.; Huang, H.; Li, Z. B.; Sun, Z. B.; Xu, Y. H.; Xiao, Q. L.; Yu, X. F.; Zhao, Y. T.; Zhang, H.; Wang, H. Y.; Chu, P. K. Biodegradable Black Phosphorus-Based Nanospheres for *in Vivo* Photothermal Cancer Therapy. *Nat. Commun.* **2016**, *7*, 12967.

(5) Zhao, Y. T.; Wang, H. Y.; Huang, H.; Xiao, Q. L.; Xu, Y. H.; Guo, Z. N.; Xie, H. H.; Shao, J. D.; Sun, Z. B.; Han, W. J.; Yu, X. F.; Li, P. H.; Chu, P. K. Surface Coordination of Black Phosphorus for Robust Air and Water Stability. *Angew. Chem., Int. Ed.* **2016**, *55*, 5003-5007.

(6) Qiu, M.; Wang, D.; Liang, W. Y.; Liu, L. P.; Zhang, Y.; Chen, X.; Sang, D. K.; Xing, C. Y.; Li, Z. J.; Dong, B. Q.; Xing, F.; Fan, D. Y.; Bao, S. Y.; Zhang, H.; Cao, Y. H. Novel Concept of the Smart NIR-Light-Controlled Drug Release of Black Phosphorus Nanostructure for Cancer Therapy. *Proc. Natl. Acad. Sci. U.S.A.* **2018**, *115*, 501-506.

(7) Song, G. S.; Hao, J. L.; Liang, C.; Liu, T.; Gao, M.; Cheng, L.; Hu, J. Q.; Liu, Z. Degradable Molybdenum Oxide Nanosheets with Rapid Clearance and Efficient Tumor Homing Capabilities as a Therapeutic Nanoplatform. *Angew. Chem., Int. Ed.* **2016**, *55*, 2122-2126.

(8) Ma, N.; Zhang, M. K.; Wang, X. S.; Zhang, L.; Feng, J.; Zhang, X. Z. NIR Light-Triggered Degradable $MoTe_2$ Nanosheets for Combined Photothermal and Chemotherapy of Cancer. *Adv. Funct. Mater.* **2018**, *28*, 1801139.

(9) Liu, Y. X.; Jia, Q.; Guo, Q. W.; Wei, W.; Zhou, J. Simultaneously Activating Highly Selective Ratiometric MRI and Synergistic Therapy in Response to Intratumoral Oxidability and Acidity. *Biomaterials* **2018**, *180*, 104-116.

(10) Yun, T. Y.; Liu, Y. X.; Yi, S. Q.; Jia, Q.; Liu, Y.; Zhou, J. Artificially Controlled Degradable Nanoparticles for Contrast Switch MRI and Programmed Cancer Therapy. *Int. J. Nanomed.* **2018**, *13*, 6647-6659.

(11) Chen, Y. Y.; Cheng, L.; Dong, Z. L.; Chao, Y.; Lei, H. L.; Zhao, H.; Wang, J.; Liu, Z. Degradable Vanadium Disulfide Nanostructures with Unique Optical and Magnetic Functions for Cancer Theranostics. *Angew. Chem., Int. Ed.* **2017**, *56*, 12991-12996.

(12) Tai, Y. W.; Chiu, Y. C.; Wu, P. T.; Yu, J. S.; Chin, Y. C.; Wu, S. P.; Chuang, Y. C.; Hsieh, H. C.; Lai, P. S.; Yu, H. P.; Liao, M. Y. Degradable NIR-PTT Nanoagents with a Potential Cu@Cu_2O@polymer structure. *ACS Appl. Mater. Interfaces* **2018**, *10*, 5161-5174.

(13) Chen, L.; Feng, Y. H.; Zhou, X. J.; Zhang, Q. Q.; Nie, W.; Wang, W. Z.; Zhang, Y. Z; He, C. L. One-Pot Synthesis of MoS_2 Nanoflakes with Desirable Degradability for Photothermal Cancer Therapy. *ACS Appl. Mater. Interfaces* **2017**, *9*, 17347-17358.

(14) Guan, G. Q.; Wang, X.; Li, B.; Zhang, W. L.; Cui, Z.; Lu, X. W.; Zou, R. J.; Hu, J. Q. "Transformed" Fe_3S_4 Tetragonal Nanosheets: a High-Efficiency and Body-Clearable Agent for

Magnetic Resonance Imaging Guided Photothermal and Chemodynamic Synergistic Therapy. *Nanoscale* **2018**, *10*, 17902-17911.

(15) Choi, H. S.; Liu, W.; Misra, P.; Tanaka, E.; Zimmer, J. P.; Ipe, B. I.; Bawendi, M. G.; Frangioni, J. V. Renal Clearance of Quantum Dots. *Nat. Biotechnol.* **2007**, *25*, 1165-1170.

(16) Nel, A. E.; Madler, L.; Velegol, D.; Xia, T.; Hoek, E. M. V.; Somasundaran, P.; Klaessig, F.; Castranova, V.; Thompson, M. Understanding Biophysicochemical Interactions at the Nano-Bio Interface. *Nat. Mater.* **2009**, *8*, 543-557.

(17) Yang, G. B.; Phua, S. Z. F.; Bindra, A. K.; Zhao, Y. L. Degradability and Clearance of Inorganic Nanoparticles for Biomedical Applications. *Adv. Mater.* **2019**, *31*, 1805730.